Letter

Reduction of the collective dynamics of neural populations with realistic forms of heterogeneity

Vladimir Klinshov, Sergey Kirillov, and Vladimir Nekorkin
Institute of Applied Physics of the Russian Academy of Sciences, 46 Ul'yanov Street, 603950 Nizhny Novgorod, Russia

(Received 2 February 2021; accepted 16 March 2021; published 20 April 2021)

Reduction of collective dynamics of large heterogeneous populations to low-dimensional mean-field models is an important task of modern theoretical neuroscience. Such models can be derived from microscopic equations, for example with the help of Ott-Antonsen theory. An often used assumption of the Lorentzian distribution of the unit parameters makes the reduction especially efficient. However, the Lorentzian distribution is often implausible as having undefined moments, and the collective behavior of populations with other distributions needs to be studied. In the present Letter we propose a method which allows efficient reduction for an arbitrary distribution and show how it performs for the Gaussian distribution. We show that a reduced system for several macroscopic complex variables provides an accurate description of a population of thousands of neurons. Using this reduction technique we demonstrate that the population dynamics depends significantly on the form of its parameter distribution. In particular, the dynamics of populations with Lorentzian and Gaussian distributions with the same center and width differ drastically.

DOI: 10.1103/PhysRevE.103.L040302

Large networks of interacting neurons may demonstrate quite a rich repertoire of collective behavior, including synchronization and collective oscillations [1,2], multistability [3–5], collective irregular dynamics and chaos [6–8], transient activity [9–11], and spatiotemporal patterns [12,13]. A long-standing task in theoretical neuroscience is obtaining reduced models describing the collective dynamics of large neural populations in terms of low-dimensional dynamical systems for averaged variables [14–16]. Such mean-field models or neuron mass models can be obtained heuristically or derived analytically from the equations for microscopic dynamics. In the latter directions, several approaches have been developed, including the refractory density method [17,18], the master equation formalism [19–21], the Ott-Antonsen ansatz [22–25], and the Lorentzian ansatz [26–28].

The latter two closely related methods allow us to obtain mean-field equations for populations of all-to-all coupled neurons which are exact in the thermodynamic limit. The reduction turns out to be especially effective for heterogeneous populations with the Lorentzian (Cauchy) distribution of internal parameters of the neurons. For such distributions, use of the residue theory allows us to reduce the population dynamics to just a single equation for a complex order parameter. However, a sufficient drawback is that the first and higher moments of the Lorentzian distribution are undefined, which makes it uncommon for realistic systems. Although one can consider the Lorentzian distribution as paradigmatic, it remains unclear how precisely it approximates the dynamics of populations with more plausible distributions of parameters. Below we show that the difference can be striking even for distributions with the same mean and width. Therefore obtaining and studying efficient mean-field models for populations with realistic forms of heterogeneity (i.e., distributions of parameters) remains an important problem.

In the current Letter we address this problem by studying a population of quadratic integrate-and-fire neurons with a Gaussian distribution of bias currents. Note that the Gaussian distribution is chosen only as an example, and our approach is applicable for arbitrary distributions as well. Although the probability density function of the Gaussian distribution does not allow us to use the residue theory directly, we construct a series of approximating distributions in the form of rational functions which allow us to overcome this limitation and so to perform the reduction of the population dynamics. The higher the dimension of the reduced system, the better it reproduces the dynamics of the original one, and 5–10 equations for complex variables turn out to be enough to approximate a population of as many as 10^4 neurons. Our results reveal that the populations with Lorentzian and Gaussian distribution are quite different in terms of both asymptotic and transient dynamics. This observation further underlines the importance of developing reduction approaches for populations with various forms of heterogeneity.

As the basic model we consider a network of quadratic integrate-and-fire neurons

$$\dot{V}_j = V_j^2 + \eta_j + Js(t) + I(t), \tag{1}$$

where V_j is the membrane potential of the j neuron, η_j is a heterogeneous component of the external current, $I(t)$ is a common time-dependent component of the external input, J is the synaptic weight, and $s(t)$ is the normalized output signal of the network. Each time a potential V_j reaches the threshold value V_p, it is reset to the value V_r, and the neuron emits a spike which contributes to the network output:

$$s(t) = \frac{1}{N}\sum_{j=1}^{N}\sum_{k}\delta_\alpha(t' - t_j^k), \tag{2}$$

where t_j^k is the moment of the kth spike of the jth neuron, and $\delta_\alpha(t) = \chi(t)\alpha e^{-\alpha t}$ [$\chi(\cdot)$ being the Heaviside function] describes the contribution of a single spike. Further, we consider the limit $\alpha \to \infty$, for which $\delta_\alpha(t)$ becomes the Dirac delta function $\delta(t)$. We also set $V_p = -V_r = \infty$ since the quadratic nonlinearity on the right-hand side of (1) allows V_j to reach infinity in a finite time.

Recently, Montbrió *et al.* [26] suggested a method for reduction of a system (1) which we briefly reproduce below. In the thermodynamic limit $N \to \infty$, the probability density function $g(\eta)$ can be introduced to describe the parameter distribution. The population state is then characterized by the density function $\rho(V|\eta, t)$ which evolves according to the continuity equation

$$\partial_t \rho + \partial_V[(V^2 + \eta + Js + I)\rho] = 0. \tag{3}$$

Assuming that solutions of (3) generically converge to a Lorentzian-shaped function

$$\rho_0(V|\eta) = \frac{1}{\pi}\frac{x(\eta, t)}{[V - y(\eta, t)]^2 + x(\eta, t)^2}, \tag{4}$$

it is possible to reduce PDE (3) to an ODE

$$\partial_t w(\eta, t) = i[\eta + Js(t) - w(\eta, t)^2 + I(t)], \tag{5}$$

where $w(\eta, t) \equiv x(\eta, t) + iy(\eta, t)$ is a complex variable characterizing the voltage distribution of neurons with a given η. The firing rate for each η value is given by the probability flux through the threshold: $r(\eta, t) = \rho(V_p, t)\dot{V}(V_p, t) = x(\eta, t)/\pi$. Then the network output $s(t)$ becomes its mean firing rate

$$r(t) = \frac{1}{\pi}\,\mathrm{Re}\int_{-\infty}^{\infty} w(\eta, t)g(\eta)d\eta, \tag{6}$$

which makes (5) a closed set of integro-differential equations. It is valid for an arbitrary distribution $g(\eta)$ but becomes especially effective for the Lorentzian distribution

$$g_L(\eta) = \frac{1}{\pi}\frac{\Delta}{(\eta - \bar{\eta})^2 + \Delta^2}, \tag{7}$$

where $\bar{\eta}$ is the mean, and Δ the half-width of the distribution [29]. For such a distribution, the integral in Eq. (6) can be evaluated using the residue theory. Namely, function $w(\eta, t)$ is analytically continued into a complex-valued η, and the integration contour is closed in the lower half-plane. Since $g_L(\eta)$ has only one pole $\eta_1 = \bar{\eta} - i\Delta$ in this half-plane, the integral (6) depends only on $w_1 = w(\bar{\eta} - i\Delta, t)$. Then $r(t) = \mathrm{Re}\, w_1/\pi$, and substituting η_1 into (5) one obtains

$$\dot{w}_1 = i[\eta_1 + J\,\mathrm{Re}\, w_1/\pi - w_1^2 + I(t)]. \tag{8}$$

Dividing the real and the imaginary parts leads to a system of two coupled ODEs

$$\dot{r} = \Delta/\pi + 2rv, \tag{9a}$$

$$\dot{v} = v^2 + \bar{\eta} + Jr - \pi^2 r^2 + I(t), \tag{9b}$$

where $v = \mathrm{Im}\, w_1$ turns out to be the mean membrane potential of the population (see Ref. [26] for details). Thus, system (1) completely describes the macroscopic dynamics of population (1) in terms of physically meaningful averaged variables r and v.

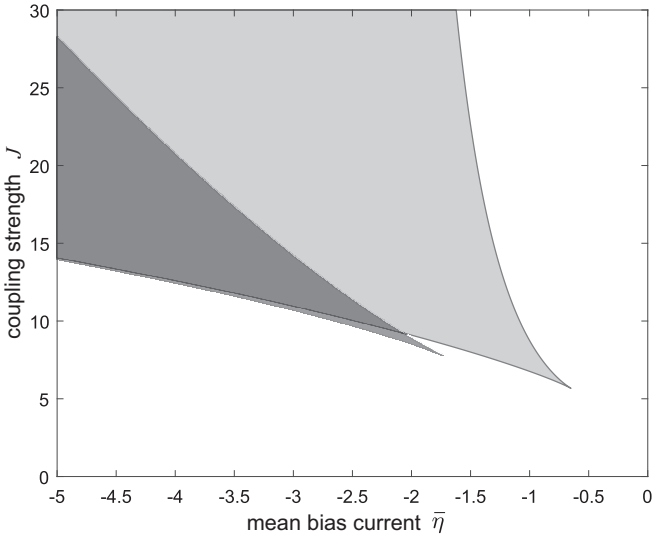

FIG. 1. Bistability regions of the population with Gaussian (light gray) and Lorentzian (dark gray) distribution of bias currents. Both distributions have the same mean and width.

The possibility to use the residue theorem and to sharply reduce the system dimension makes the Lorentzian distribution quite popular in studies of heterogeneous populations not only in neuroscience, but also in other fields of nonlinear dynamics [30–32]. However, despite the analysis simplification it leads to, this distribution is physically implausible since all its moments are not well defined. Therefore it is important to understand whether the replacement of the Lorentzian distribution by more realistic distributions leads to significant changes in the population dynamics. In order to tackle this issue we consider a Gaussian distribution of the quenched components η:

$$g_G(\eta) = \frac{1}{\sigma\sqrt{2\pi}}e^{-\frac{(\eta-\bar{\eta})^2}{2\sigma^2}}. \tag{10}$$

The Gaussian distribution is typical for many physical variables, and in many cases it is a good approximation for some other distributions, such as binomial. Further we set $\sigma = 1$.

First let us study the autonomous dynamics of the populations with $I(t) = 0$. The numerical analysis of the full population of size $N = 10^4$ with the Gaussian parameter distribution reveals that the dynamics is qualitatively similar to those for the Lorentzian distribution, as already was pointed in Ref. [26] (where both cases were considered). Depending on the mean bias current $\bar{\eta}$ and the coupling strength J, the system may demonstrate low-activity and high-activity states, with a wedge-shaped bistability region bounded by two saddle-node bifurcation curves. However, the exact positions of the bistability regions are quite different for the Gaussian and the Lorentzian distributions as illustrated in Fig. 1. Further we will show how to reduce the population with the Gaussian distribution to a low-dimensional dynamical system similar to (9).

Although Eq. (5) remains valid for the Gaussian distribution, the residue theorem does not allow us to evaluate the integral in Eq. (6) since $g_G(\eta)$ does not fade for $\mathrm{Im}\,\eta \to \infty$. A possible solution is to approximate the Gaussian distribution

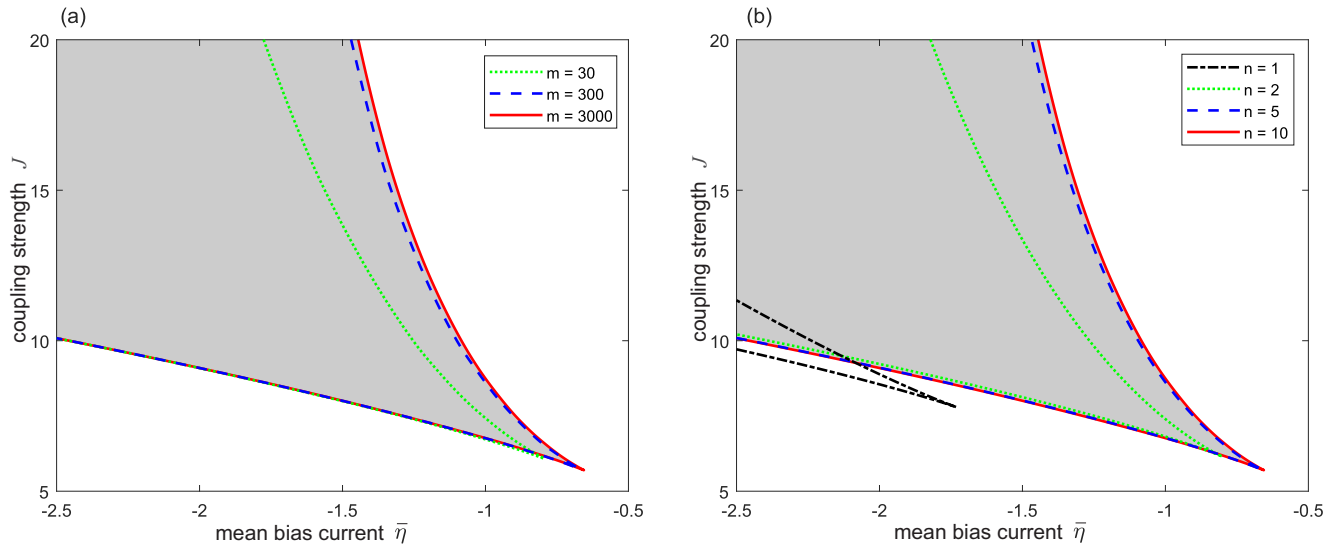

FIG. 2. Bifurcation diagram of the population with Gaussian distribution of bias currents and its approximations. Shaded area in (a) and (b) depicts the bistability region of the full population with $N = 10^4$ neurons. In (a), the borders of the same region obtained from the interval approximation are superimposed for $m = 30$ (green dotted line), $m = 300$ (blue dashed line), and $m = 3000$ (red solid line). In (b), the borders obtained from the rational approximation are shown for $n = 1$ (black dash-dotted line), $n = 2$ (green dotted line), $n = 5$ (blue dashed line), and $n = 10$ (red solid line).

by a sum of sharp Lorentzian functions, each of them approximating a small fraction of the population with η in a narrow interval of width ϵ:

$$g(\eta) \approx \sum_{k=1}^{m} g_G(\eta_k) \frac{1}{\pi} \frac{\epsilon}{(\eta - \eta_k)^2 + \epsilon^2}. \tag{11}$$

Here, m is the number of intervals, and the points η_k are uniformly distributed so that $\eta_k = \bar{\eta} - L + \epsilon(k - 1/2)$, where $2L = m\epsilon \gg \sigma$. Then the population dynamics is reduced to a set of systems of form (9) for m subpopulations coupled through their mean firing rate:

$$r = \frac{1}{\pi} \mathrm{Re} \sum_{k=1}^{m} g_G(\eta_k) w_k. \tag{12}$$

An important disadvantage of the interval approximation (11) is that it adequately represents the original distribution only when the number of intervals m is very large. Consequently, system (12) becomes highly dimensional, and the reduction loses its effectiveness. Figure 2(a) shows that the reduced system accurately reproduces the phase diagram of the original population for $m = 3000$ parameter intervals, but fails for as many as $m = 300$ intervals.

In order to develop more efficient methods of the dynamics reduction we suggest another approximation of the Gaussian distribution. The main idea is to use the approximation allowing the evaluation of the integral in Eq. (6) with the help of the residue theory but having only a few poles. We use a series of approximations in the form of rational functions. To obtain them we replace the exponential function in Eq. (10) by the Taylor series

$$e^{x^2} \approx h_n(x) = \sum_{k=0}^{n} \frac{1}{k!} x^{2k}, \tag{13}$$

which leads to the following approximation:

$$g_n(\eta) = \frac{\gamma_n}{\sigma_n \sqrt{2\pi}} \left[h_n\left(\frac{\eta - \bar{\eta}}{\sigma_n \sqrt{2}} \right) \right]^{-1}. \tag{14}$$

Here, γ_n is the normalization factor, and σ_n is chosen such that the half-width of the approximating distributions is equal for all n (this was done in order to facilitate the comparison between different distributions). The sequence of functions g_n converges to g_G (although not uniformly), as illustrated in Fig. 3. At the same time, $g_n(\eta) \sim \eta^{-2n}$ for large η, which allows us to close the integration contour in Eq. (6) by an (infinitely large) arc in the lower half-plane of complex-valued η.

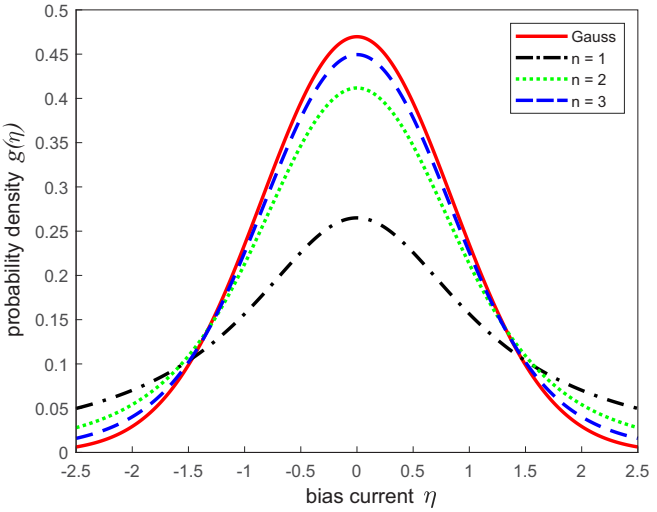

FIG. 3. Gaussian distribution (red solid line) and its rational approximations (14) for $n = 1$ (black dash-dotted line), $n = 2$ (green dotted line), and $n = 3$ (blue dashed line).

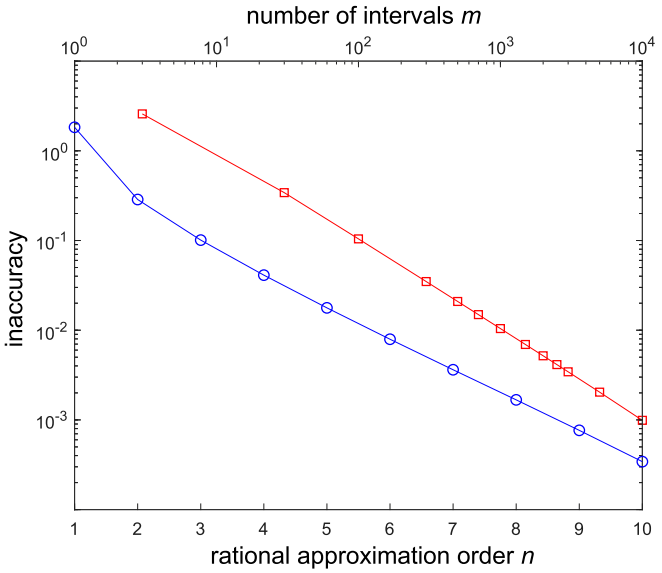

FIG. 4. The inaccuracy of the bifurcation prediction versus the number of intervals m for the interval approximation (red line with boxes) and the approximation order n for the rational approximation (blue line with circles). The parameter $J = 15$ was fixed, and the bifurcation value of $\bar{\eta}$ was determined. Note the significant difference in the horizontal axis scale for the two approximations.

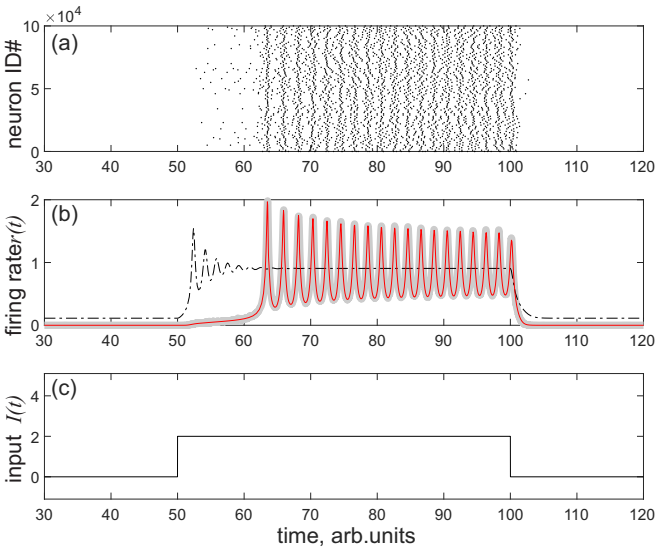

FIG. 5. The dynamics of the full population and its approximations. (a) Raster plot of 100 randomly chosen neurons. (b) The firing rate of the whole population (thick gray line) and its rational approximation with $n = 10$ (thin red line) and $n = 1$ (Lorentzian approximation, black dot-dashed line). (c) The input signal. The system parameters are $N = 10^4$, $J = 10$, $\bar{\eta} = -3$; the parameters of the input signal are $t_0 = 50$, $T = 50$, and $A = 2$.

Then the integral depends only on the values $w_k = w(\eta_k, t)$, where η_k are the zeros of $h_n(\eta)$ with $\mathrm{Im}\,\eta_k < 0$. Taking into account that there are exactly n such points and calculating the residues of g_n at η_k we obtain

$$r = \gamma_n 2^n \sigma_n^{2n+1} n! \sqrt{\frac{2}{\pi}}\,\mathrm{Re}\left(i \sum_{k=1}^{n} \frac{w_k}{(\eta_k - \bar{\eta})^{2n+1}}\right). \tag{15}$$

Then Eq. (5) reduces to a set of n ODEs

$$\dot{w}_k = i\left[\eta_k + Jr - w_k^2 + I(t)\right], \quad k = 1, \ldots, n. \tag{16}$$

Along with (15), system (16) provides a complete description of the macroscopic behavior of the population. The rational approximation becomes quite accurate already for $n > 3$; therefore one should expect good agreement between the reduced system and the full population even for small n. In order to check this hypothesis we carried out the bifurcation analysis of system (16) for various n. In Fig. 2(b), the obtained bifurcation curves are superimposed on the phase diagram of the full population. The agreement is remarkable already for $n = 10$ which is several orders less than for the interval approximation.

To better illustrate the advantage of the rational approximation approach, we compared the accuracy of the bifurcation prediction for both approximations. For this sake we fixed $J = 15$ and calculated the value of $\bar{\eta}$ corresponding to the saddle-node bifurcation. In Fig. 4, the prediction inaccuracy is plotted versus the number of intervals m for the interval approximation and the approximation order n for the rational approximation. Note the significant difference in the horizontal scale for the two approaches. For both cases, the error vanishes as the approximation order increases, but the decay rate is significantly different. For example, in order to obtain the accuracy $\varepsilon < 10^{-2}$ one needs just $n = 6$ for the rational approximation, but as many as $n = 1000$ for the interval one. To decrease the error twice, it is enough to increase the order of the rational approximation by 1, while the order of the interval approximation should be increased almost twice.

We have demonstrated that the rational approximation allows us to obtain low-dimensional reduced systems accurately reproducing the phase diagram of the population. However, the bifurcation analysis allows us to study only asymptotic behavior, whereas neuronal populations must rapidly react on changing external stimuli. Thus, their transient dynamics is of high importance. In order to test the efficiency of the reduced system for their reproduction, we consider a pulse-like input signal

$$I(t) = A[\chi(t - t_0) - \chi(t - t_0 - T)], \tag{17}$$

where A is the pulse amplitude, t_0 is its starting moment, and T its duration. We fixed the signal parameters and simulated the population 20 times starting from random initial conditions (the initial voltage was set randomly and independently for each neuron). For all the trials, the macroscopic dynamics rapidly converged to the same trajectory, and the raster plots of most of the neurons converged to the same pattern as well [33]. This observation corroborates the stability of the Lorentzian manifold (4).

Figure 5 compares the dynamics of the original population and two rational approximations with $n = 1$ and $n = 10$. The first-order approximation is in fact a Lorentzian fit of the Gaussian distribution which poorly approximates the latter (see Fig. 3). Figure 5(b) shows the time trace of the population firing rate; a moving average filter with the width $\tau = 0.01$ was used in order to smooth out individual spikes. When the

stimulus is applied, the firing rate of the population temporally grows, and goes down to the initial low value when the stimulation is over. Interestingly enough, the response of the population turns out to be delayed: it takes about 10 time units from the beginning of the pulse for the firing rate to start increasing. Another important feature is that the response is strongly synchronized which is reflected in pronounced oscillations of the firing rate. The Lorentzian approximation fails to reproduce these important effects, while the rational approximation with $n = 10$ captures them quite accurately [34].

The results presented in this Letter reveal significant difference between the dynamics of populations with different forms of heterogeneity. Although the mean and the width are equal for the Gaussian distribution and for its Lorentzian fit, they induce different collective behavior of the population. The difference is both in asymptotic and transient dynamics, which means that the particular form of the population heterogeneity is crucial for its dynamical properties. Therefore it is important to develop mean-field models for populations with not only paradigmatic Lorentzian distribution of parameters, but with more realistic distributions as well.

Our solution to this problem is the method of rational approximations which allows us to obtain reduced systems for populations with a given distribution. Note that this method is not limited to the Gaussian distribution but applicable to an arbitrary distribution $g(\cdot)$ which can be approximated by a series of rational functions $g_n(\cdot)$, such as Padé approximants [35], Chebyshev-Padé approximants [36], or some others. As soon as such an approximation is obtained, a reduced system in the form of Eqs. (15) and (16) can be readily derived and used to study the collective dynamics of the population.

The research was supported by the Russian Science Foundation (Grant No. 19-72-10114). The authors are grateful to Diego Pazó for reading the manuscript and useful comments.

[1] R. E. Mirollo and S. H. Strogatz, SIAM J. Appl. Math. **50**, 1645 (1990).
[2] S. M. Crook, G. B. Ermentrout, and J. M. Bower, Neural Comput. **10**, 837 (1998).
[3] A. Renart, N. Brunel, and X.-J. Wang, *Computational Neuroscience: A Comprehensive Approach* (Chapman and Hall/CRC Press, London, UK, 2004).
[4] V. V. Klinshov, J.-n. Teramae, V. I. Nekorkin, and T. Fukai, PLoS One **9**, e94292 (2014).
[5] P. So, T. B. Luke, and E. Barreto, Physica D **267**, 16 (2014).
[6] S. Olmi, A. Politi, and A. Torcini, Europhys. Lett. **92**, 60007 (2010).
[7] D. Pazó and E. Montbrió, Phys. Rev. Lett. **116**, 238101 (2016).
[8] A. Politi, E. Ullner, and A. Torcini, Eur. Phys. J.: Spec. Top. **227**, 1185 (2018).
[9] O. V. Maslennikov, D. S. Shchapin, and V. I. Nekorkin, Philos. Trans. R. Soc. London A **375**, 20160288 (2017).
[10] R. F. O. Pena, M. A. Zaks, and A. C. Roque, J. Comput. Neurosci. **45**, 1 (2018).
[11] C. C. A. Fung and T. Fukai, Sci. Rep. **8**, 10680 (2018).
[12] M. R. Tinsley, S. Nkomo, and K. Showalter, Nat. Phys. **8**, 662 (2012).
[13] C. R. Laing and O. Omel'chenko, Chaos **30**, 43117 (2020).
[14] T. Schwalger and A. V. Chizhov, Curr. Opin. Neurobiol. **58**, 155 (2019).
[15] S. Coombes and Á. Byrne, *Nonlinear Dynamics in Computational Neuroscience* (Springer, Cham, Switzerland, 2019), pp. 1–16.
[16] C. Bick, M. Goodfellow, C. R. Laing, and E. A. Martens, J. Math. Neurosci. **10**, 9 (2020).
[17] W. Gerstner, Neural Comput. **12**, 43 (2000).
[18] T. Schwalger, M. Deger, and W. Gerstner, PLoS Comput. Biol. **13**, e1005507 (2017).
[19] C. Van Vreeswijk and H. Sompolinsky, Neural Comput. **10**, 1321 (1998).
[20] S. El Boustani and A. Destexhe, Neural Comput. **21**, 46 (2009).
[21] M. Di Volo, A. Romagnoni, C. Capone, and A. Destexhe, Neural Comput. **31**, 653 (2019).
[22] E. Ott and T. M. Antonsen, Chaos **18**, 37113 (2008).
[23] E. Ott and T. M. Antonsen, Chaos **19**, 23117 (2009).
[24] T. B. Luke, E. Barreto, and P. So, Neural Comput. **25**, 3207 (2013).
[25] C. R. Laing, Phys. Rev. E **90**, 010901(R) (2014).
[26] E. Montbrió, D. Pazó, and A. Roxin, Phys. Rev. X **5**, 021028 (2015).
[27] I. Ratas and K. Pyragas, Phys. Rev. E **94**, 032215 (2016).
[28] M. di Volo and A. Torcini, Phys. Rev. Lett. **121**, 128301 (2018).
[29] Here and further, the "mean" of the Lorentzian distribution is calculated as the Cauchy principal value p.v.$\int_{-\infty}^{\infty} f(x)dx = \lim_{a\to\infty}\int_{-a}^{a} f(x)dx$.
[30] E. A. Martens, E. Barreto, S. Strogatz, E. Ott, P. So, and T. M. Antonsen, Phys. Rev. E, **79**, 026204 (2009).
[31] A. Pikovsky and M. Rosenblum, Physica D **240**, 872 (2011).
[32] D. S. Goldobin, I. V. Tyulkina, L. S. Klimenko, and A. Pikovsky, Chaos **28**, 101101 (2018).
[33] The convergence of individual spiking patterns is not observed only for neurons with a high bias current $\eta_j > 0$ which remain oscillatory even in the absence of the external input I.
[34] Note that although the oscillations of the firing rate during the input look periodic, in reality they are damped with a very small decrement. The oscillations dying out can be seen when long inputs with $T \sim 1000$ are applied (data not shown).
[35] H. Padé, Ann. Sci. l'École Norm. Super. **9**, 3 (1892).
[36] L. N. Trefetlien, in *Algorithms for Approximation*, edited by J. Mason and M. Cox (Clarendon Press, Oxford, 1987), pp. 227–264.